HAL
open science

Multigrid motion estimation on pyramidal representations for image sequence coding

Nadia Baaziz, Claude Labit

To cite this version:

Nadia Baaziz, Claude Labit. Multigrid motion estimation on pyramidal representations for image sequence coding. [Research Report] RR-1409, INRIA. 1991. inria-00075151

HAL Id: inria-00075151

https://inria.hal.science/inria-00075151v1

Submitted on 24 May 2006

HAL is a multi-disciplinary open access archive for the deposit and dissemination of scientific research documents, whether they are published or not. The documents may come from teaching and research institutions in France or abroad, or from public or private research centers.

L'archive ouverte pluridisciplinaire **HAL**, est destinée au dépôt et à la diffusion de documents scientifiques de niveau recherche, publiés ou non, émanant des établissements d'enseignement et de recherche français ou étrangers, des laboratoires publics ou privés.

UNITÉ DE RECHERCHE
INRIA RENNES

Institut National
de Recherche
en Informatique
et en Automatique

Domaine de Voluceau
Rocquencourt
BP 105
78153 Le Chesnay Cedex
France
Tél (1) 39 63 55 11

Rapports de Recherche

N° 1409

Programme 4
Robotique, Image et Vision

MULTIGRID MOTION ESTIMATION ON PYRAMIDAL REPRESENTATIONS FOR IMAGE SEQUENCE CODING

Nadia BAAZIZ
Claude LABIT

Avril 1991

RR.1409

IRISA INSTITUT DE RECHERCHE EN INFORMATIQUE ET SYSTEMES ALEATOIRES

Campus Universitaire de Beaulieu
35042 - RENNES CEDEX
FRANCE
Téléphone : 99.36.20.00
Télex : UNIRISA 950 473F
Télécopie : 99.38.38.32

Multigrid motion estimation on pyramidal representations for image sequence coding

Nadia BAAZIZ, Claude LABIT
IRISA/INRIA, Campus de Beaulieu 35042 Rennes Cedex, France
Tel: 99 36 20 00 Telex: UNIRISA 950 473 F
FAX: 99 38 38 32

Publication Interne n° 572 - 48 pages
Février 1991 - Programme 4

Abstract

This paper investigates the efficiency of several multigrid motion estimation schemes to improve image sequence coding using motion compensated predictions. In two different and isolated contexts of applications, some previous studies proved the interest to design hierarchical and compact representation for image data (lowpass pyramids, QMF and/or wavelet decompositions...) applied to one spatial image and, moreover, some numerous experiments and codec designs have already used motion compensated prediction loops. The outlines of this paper are to take advantage of a hierarchical decomposition to build efficient motion estimator simultaneously in several frequency bands. Usual differential estimation methods are experimented on lowpass pyramids and wavelet pyramids with several merging operators. A modified Wiener-based motion estimator is presented and improves the motion estimation efficiency within an orthogonal oriented image decomposition. Finally, results are shown and compared on real television image sequences.

CENTRE NATIONAL DE LA RECHERCHE SCIENTIFIQUE
(U.R.A. 227)
UNIVERSITE DE RENNES I I.N.S.A. DE RENNES

INSTITUT NATIONAL DE RECHERCHE
EN INFORMATIQUE ET EN AUTOMATIQUE
(UNITE DE RECHERCHE DE RENNES)

Estimation de mouvement multigrille sur des

Représentations pyramidales

Pour le codage de séquences d'images

Résumé

Ce travail consiste à tester l'efficacité de différentes stratégies multigrilles d'estimation de mouvement pour l'amélioration de techniques de codage de séquences d'images par compensation de mouvement. Dans deux contextes différents, des travaux antécédents ont montré l'utilité de concevoir des représentations hiérarchiques et compactes d'images numériques (Pyramides passebas, décompositions QMF et/ou ondelettes ...). Par ailleurs, plusieurs expérimentations ont été menées par la mise en œuvre de schémas de codage utilisant des boucles de prédiction par compensation de mouvement. Le but de ce travail est d'exploiter les avantages des représentations hiérarchiques dans la conception d'un estimateur de mouvement efficace. Quelques estimateurs de mouvements appartenant à la famille des méthodes différentielles sont expérimentés sur des pyramides passebas et des pyramides ondelettes en leur associant des stratégies multigrilles et des opérateurs de fusion. Une version modifiée de l'estimateur de Wiener est présentée, son efficacité à s'adapter à une décomposition orthogonale orientée est montrée. Des résultats comparatifs et relatifs à des séquences d'images télévisuelles réelles sont donnés.

Contents

1 Introduction **2**

2 Multiresolution representations of image sequences **3**

2.1 Lowpass pyramid transforms 6

2.2 Non-orthogonal pyramid transforms 6

2.3 Orthogonal bandpass pyramid transforms 11

2.3.1 Introduction 11

2.3.2 Wavelet pyramids 11

2.4 Quasi-orthogonal pyramid transforms 17

2.4.1 Introduction 17

2.4.2 The quincunx pyramid 17

2.5 Discussion 19

3 Motion estimation framework **21**

3.1 Adaptive pel-recursive motion estimation algorithm 21

3.2 Wiener-based algorithm 22

3.3 Modified Wiener-based approach 23

4 Multigrid motion estimation **27**

4.1 Multigrid Walker-Rao algorithm on lowpass pyramids 27

4.2 Multigrid Walker-Rao algorithm on wavelet pyramids 29

5 Multiconstraint algorithm **31**

6 Discussion **35**

1 Introduction

Multiresolution representations have been fruitfully introduced in image processing and image data compression; indeed they perform much better in comparison with the usual transform techniques (FFT,DCT ...) which are poor in spatial-frequency localization and introduce blocking effects. Multiresolution transforms are also known as subband decomposition techniques or pyramid transforms [VET84], [WOO86], [BUR83] . Each of them have been developped separately and formulatted with different mathematical tools. The wavelet transform and the associated multiresolution analysis as it has been introduced [MEY87], [DAU87],[MAL89] relate all these techniques by associating a mathematical framework giving efficient modeling and interpretation tools for space-frequency pyramidal decomposition.
Our study mainly investigates how all these pyramidal representation schemes work with spatio-temporal (3-D) data information (i.e image sequences indexed by two (x,y) spatial components and one time axis) ; when such a hierarchical representation is applied, we can observe that the visual appearance of motion and spatio-temporal structures are quite interpretable and significant in terms of correlated motions within different somewhat decorrelated frequency subbands. The general goal of this study is to derive numerically this visual coherence of motions when a pyramidal representation is used as the basic data structure. Obviously the return of motion information is of great interest for coding purpose, when a motion compensated prediction loop is introduced in an interframe predictive coding scheme to obtain the best redundancy removal and associated bit rate reduction when a transmission service is involved [NET79], [WAL84] and [BIE87].

Section 2 presents a unified classification of several multiresolution representation methods which enable the design of pyramidal structures for image data. These methods have been introduced, sometimes, independently and sequentially. We think useful to compare all of them using the same criteria of entropy, reconstruction error, orthogonality, complexity and performance stability along a real TV image sequences. Then, we judge necessary to summarize in section 3 the general framework that we use, for motion estimation : it is based on differential methods which can be easily extended to hierarchical representations. Such a new algorithmic extension is proposed and tested. Section 4 and 5 present new motion estimation techniques which exploit the

basic hierarchical data structure due to any pyramidal decomposition previously introduced. Theses techniques are defined as multigrid motion estimation (section 4) and denoted by multiconstraint algorithms (section 5) if several frequency subbands are simultaneously processed.

2 Multiresolution representations of image sequences

The main outline of this section is to present a synthesized and classified typology of several (already known) pyramidal decomposition techniques which have been, in the past introduced separately and not really compared on a unique experimental set of image data and criteria. Especially, for image coding applications, we look at these techniques as pyramid transforms based essentially on filtering and decimation processes, the pyramid levels are equivalent to frequency channels with adapted bandwith and orientations. Figure 1 gives our typology tree and associated references. It is based essentially on the following classification criteria :

- Filtering nature : we can separate first of all pyramid transforms based on bandpass filtering (Laplacian pyramid, Pseudo-Laplacian pyramid, subband decompositions...) from those based only on lowpass filtering which give us several approximated versions of the original image data at successive resolutions (Gaussian pyramid, Pseudo-Gaussian pyramid, Crible).

- Orthogonality : within the family of bandpass pyramids, we distinguish three subclasses which introduce respectively a non-orthogonal representation (Laplacian pyramid, Pseudo-Laplacian pyramid, Crible), a quasi-orthogonal one which means that only a sometimes approximation of orthogonality is achieved, and finally strictly orthogonal representation.

- Separability : one traditionnal method consist to extend the use of filters designed for monodimensional (1-D) signals to multidimensional signals (2-D or more than) in a separable way. However, there are some

studies which have introduced non-separable bandpass filtering which could isolate some more isotropic patterns within successive pyramidal levels.

All the references corresponding to these classification criteria are given in figure 1. The following subsections present some technical aspects of implementation for a subset of such decompositions. We focus our attention on some representative pyramid transforms that we use in order to dress a comparison table of their performances. Different criteria are etablished to evaluate the decomposition efficiency such as the implementation complexity and spatio-frequency localization. In the point of view of data compression, we compute partial and global entropies to estimate the degree of information decorrelation obtained for each decomposition.
Since we dispose of 3-D data information (x, y, t) corresponding to television sequence, the transforms are applied to each frame to obtain a pyramid sequence.

Two sequences, especially taken for their representative contents of structures and motion features, have been used for the simulations presented here. The first sequence called "INTERVIEW"(by courtesy of BBC-UK) is a real television sequence of 32 frames. Two successive frames of it and the corresponding temporal difference are shown in figure 15. We show respectively in figure 16 the second sequence called "RUBIX" (by courtesy of CCETT-FRANCE) which is an artificial sequence of 32 frames too.

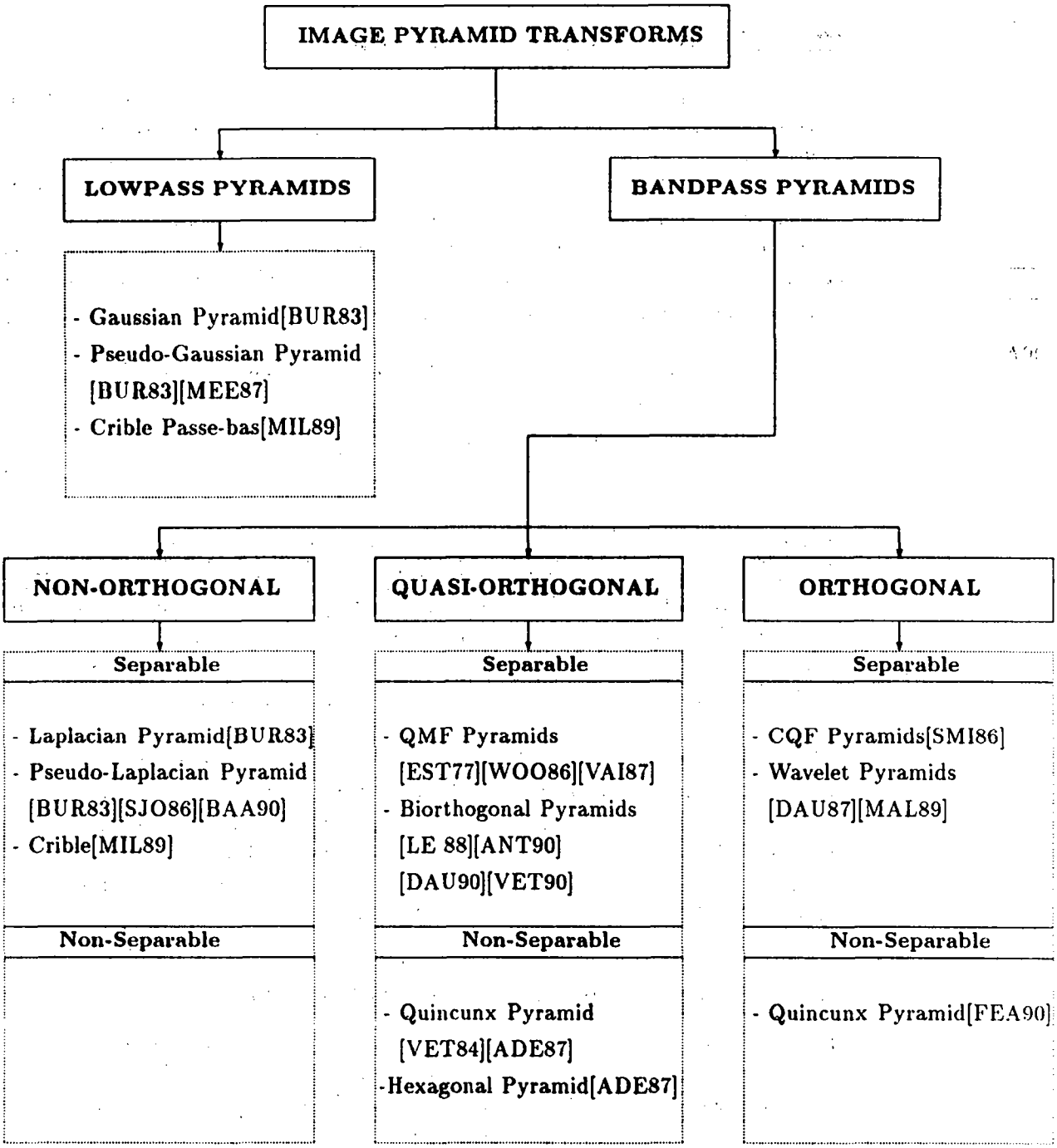

Figure 1: Typology tree of image pyramid transforms

2.1 Lowpass pyramid transforms

The most popular method belonging to this class is the Gaussian pyramid [BUR83]. In a general way, a N level lowpass pyramid (G_0,G_1,...,G_{N-1}) is a set of an original image and its approximations at a sequence of resolutions (r^{-j}) obtained by bidimensional filtering and decimation processes [MAL89]. In our case, we implement the lowpass pyramid corresponding to the approximation of the original signal at dyadic sequence of resolutions (2^{-j}), each level G_j is derived recursively from G_{j-1} by separable filtering and subsampling by a factor 2 as given by the following equations :

$$G_j(k,l) = \sum_n \sum_m h(n)h(m)G_{j-1}(2k-m, 2l-n)$$

$$-M \leq m,n \leq M$$

$$1 \leq j \leq N-1$$

where G_0 is the original image. The generating kernel h is a $(2M+1)$ tap finite impulse response of monodimensional discrete lowpass filter. A symmetry is often required to assure linear phase. The frequency bandwith is compatible with the decimation rate in respect to Shannon's theorem.
For Gaussian kernel h we obtain a Gaussian pyramid but in other case we call it a pseudo-Gaussian pyramid because it follows the same decomposition algorithm.
Since each level is a lowpass frequency partition of the higher resolution one, as it can be seen in figure 2, the resulted pyramid is a very redundant information scheme and this creates an increase of the transform sample number which attain the 4/3 of the original one. A 3 level pseudo-Gaussian pyramid of "INTERVIEW" frame is shown in figure 17, it is generated with 9 tap lowpass filter extracted from a QMF pair [ADE87].

2.2 Non-orthogonal pyramid transforms

Since lowpass pyramids are very redundant data structures, one can derive bandpass pyramids that captures only the information difference between two successive lowpass levels. If a simple difference operation is performed, the reduced level must be interpolated to have the same size than the highest resolution one. One well-known non-orthogonal bandpass pyramid was

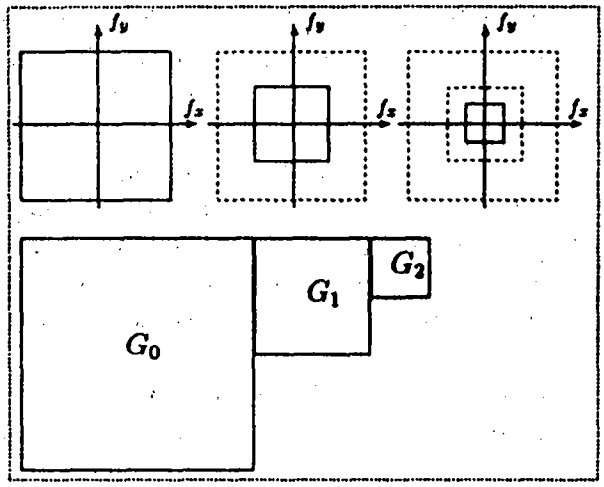

Figure 2: Spatial representation grid of a 3 level lowpass pyramid and the corresponding frequency partition.

introduced by Burt and Adelson in 1983 [BUR83] using a Gaussian pyramid. It was called the Laplacian pyramid since the difference of Gaussian kernels gives an approximation of the Laplacian of the Gaussian. For other lowpass kernels, the obtained pyramid is called a pseudo-Laplacian pyramid.
N Laplacian or pseudo-Laplacian pyramid levels $(L_0, L_1, ..., L_{N-1})$ are given by :

$$G_{j+1}(k,l) = \sum_n \sum_m h(n)h(m)G_j(2k-m, 2l-n)$$

$$\tilde{G}_{j+1}(k,l) = 4\sum_n \sum_m h(n)h(m)G_{j+1}(\frac{k+m}{2}, \frac{l+n}{2})$$

$$L_j(k,l) = G_j(k,l) - \tilde{G}_{j+1}(k,l)$$

$$L_{N-1}(k,l) = G_{N-1}(k,l)$$

$$\begin{aligned} -M &\leq m,n \leq M \\ 0 &\leq j \leq N-2 \end{aligned}$$

where G_0 is the original image and $\tilde{G}_j$ the interpolated version of a lowpass pyramid level G_j. For the filtering process, the signal may be extended out of its finite support in the simplest way in order to have easy computation.

The generating kernels can not be ideal lowpass filters, then the difference operation conserves some low-frequency energy and makes the different pyramid levels partially redundant. In other words, the transform is not orthogonal and consequently, as in the lowpass pyramid, the amount of the obtained data structure attains the 4/3 of the original image size.

In the frequency domain, the pseudo-Laplacian pyramid scheme is equivalent to a set of correlated frequency bands as it can be seen at figure 3.

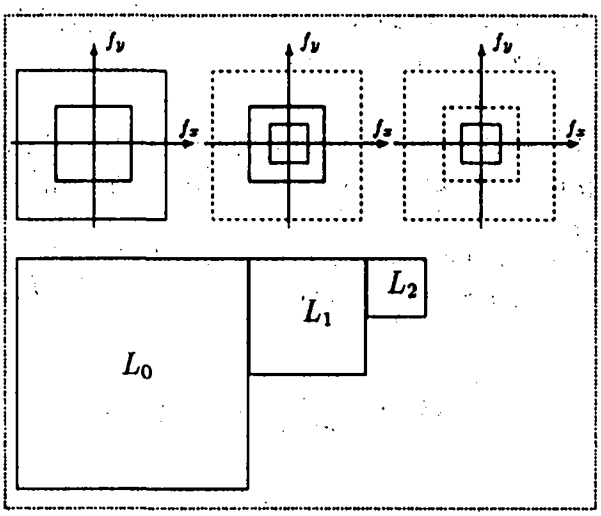

Figure 3: Spatial representation grid of a 3 level Laplacian or pseudo-Laplacian pyramid and the corresponding frequency partition.

In addition to the simplicity of the computation, the pseudo-Laplacian pyramid offers three main advantages very important in the point of view of image coding and data compression:

1) Exact reconstruction:

   The Laplacian and pseudo-Laplacian pyramids are said to be complete codes; indeed they are invertible transforms and guarantee the exact

reconstruction of the original signal. So, no artefacts occur due to the boundary effects.

The reconstruction equations are given by:

$$\begin{aligned} L_{N-1}(k,l) &= G_{N-1}(k,l) \\ G_j(k,l) &= L_j(k,l) + \tilde{G}_{j+1}(k,l) \\ 0 \leq \ j &\leq N-2 \end{aligned}$$

2) **Partial** decorrelation :

Partial and global entropy computation performed on pyramid levels shows the information decorrelation obtained by this kind of transform and outlines its advantages for coding purposes.
The global entropy E_g is given by the average of the pyramid level entropies E_{L_j} and represents the optimal number of bits required per pyramid sample in comparison with an original sample :

$$E_g = \sum_{j=0}^{N-1} \frac{E_{L_j}}{2^{2j}}$$

The entropy E of an image is defined as :

$$E = -\sum_i p_i log_2(p_i)$$

where p_i is the distribution probability of its pixel values i.

The following table gives original, partial and global entropy values for :

- "RUBIX" frame and its 3 level Laplacian pyramid generated with 5-tap Gaussian filter.
- " INTERVIEW" frame and its 3 level pseudo-Laplacian pyramid generated from 9-tap lowpass filter (see figure 17).

RUBIX frame		INTERVIEW frame	
Original	3.84	*Original*	7.51
E_{L_0}	3.31	E_{L_0}	3.83
E_{L_1}	3.43	E_{L_1}	4.44
E_{L_2}	4.01	E_{L_2}	4.47
E_g	4.42	E_g	5.22

One can notice that partial entropies have small values, this effect is quite expected in coding applications. However, such transform suffers from the non-orthogonality which makes an increase of the data amount and high global entropy.

3) Error compensation loop:

During the coding process, if such a hierarchical data representation is introduced in it, some bias or coding errors can occur : quantization errors, transmission errors, ..., propagation error due to any divergence between a coder and its dual decoder. In order to attenuate distorsion due to a propagation of these errors inside the pyramidal structure, from one level to each other, it seems fruitful to introduce an error compensation loop in the framework of pseudo-Laplacian decompositions, it is entirely described in [BAA90a], [BAA90b]. Briefly, we can notice that this technique is similar to the prediction loop design within a DPCM coding scheme where strictly speaking, only reconstructed data (i.e image data) which have been already coded and decoded are used, symmetrically at the coder and the decoder. In our case of hierarchical representation, it means that for each highpass level computation, only previously reconstructed lowpass levels are used ; this pyramid design works in a coarse-to-fine (or top-bottom) sense. So, the propagation error is minimized and the distorsion of the reconstructed image will depend essentially from the coding error of the bottom level of the pseudo-Laplacian pyramid. If the coding is only a quantization process, the introduction of error compensation method permits a significant decrease of the amount and range of reconstruction errors; however such an introduction destroys the intrinsic parallelism inside the pyramid design step.

2.3 Orthogonal bandpass pyramid transforms

2.3.1 Introduction

Orthogonal pyramid transforms correspond essentially to exact reconstruction subband coding schemes which split the image spectrum into N uncorrelated frequency channels by bandpass filtering and adapted subsampling. The original signal can be exactly reconstructed by converse operations.
The analysis/synthesis filters have the fondamental property to form an orthonormal set. Conjuguate Mirror Filters (CQF) [SMI86] and wavelet filters [DAU87] are examples of filter banks which generate this kind of pyramids.

2.3.2 Wavelet pyramids

The original image is decomposed in a set of subimages corresponding to a dyadic resolution sequence (2^{-j}) [MAL89]. This transform is implemented using a pair of non-symmetrical analysis/synthesis filters (H, G) derived from orthonormal wavelet basis with compact support [DAU87]. They are 1-D finite impulse response filters (FIR) which leads to orthogonality and exact reconstruction concepts as it can be seen through the following equations:

1- $g(n) = (-1)^n h(-n+1)$: conjuguate mirror relation.
2- $\sum_n h(n) = 1$: h is a normalized lowpass kernel. 3- $\sum_n g(n) = 0$: g is a highpass kernel. 4- $\sum_n h(n-2k)g(n-2l) = 0$: orthogonality relation.
5- $\sum_k h(m-2k)h(n-2k) + g(m-2k)g(n-2k) = \delta_{mn}$: exact reconstruction relation.
6- $\bar{h} = h(-n)$; $\bar{g} = g(-n)$.
One decomposition step gets four subimages corresponding to three oriented high frequency bands and a low frequency band. The following equations show how to combine the filters and the decimation process to get the four subbands or the first pyramid levels.

$$HH_1(k,l) = \sum_n \sum_m \bar{g}(2k-n)\bar{g}(2l-m)I_0(n,m)$$

$$HB_1(k,l) = \sum_n \sum_m \bar{g}(2k-n)\bar{h}(2l-m)I_0(n,m)$$

$$BH_1(k,l) = \sum_n \sum_m \bar{h}(2k-n)\bar{g}(2l-m)I_0(n,m)$$

$$BB_1(k,l) = \sum_n \sum_m \bar{h}(2k-n)\bar{h}(2l-m)I_0(n,m)$$

I_0 : original image.
$\bar{h}$: impulse response of lowpass wavelet filter.
$\bar{g}$: impulse response of highpass wavelet filter.
HH_1 : subimage of diagonal high frequencies, isolates diagonal edges.
HB_1 : subimage of horizontal high frequencies, isolates vertical edges.
BH_1 : subimage of vertical high frequencies, isolates horizontal edges.
BB_1 : subimage of low frequencies, represents the context of the image.

For boundary filtering, the image signal is assumed to be periodic.

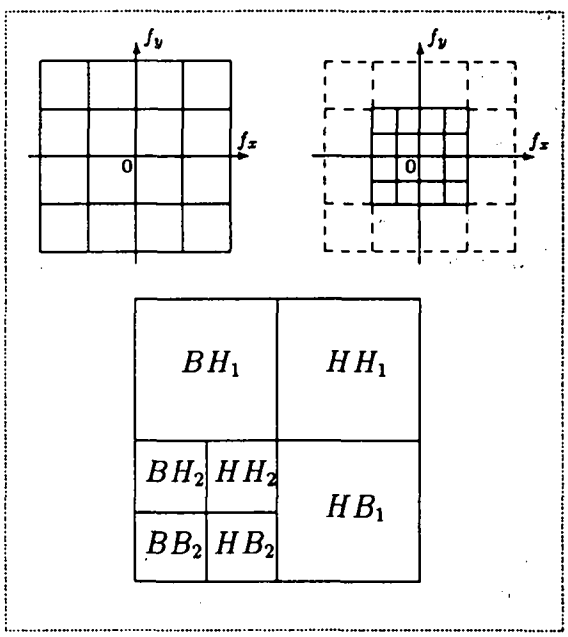

Figure 4: Spatial representation grid of a 2 level wavelet pyramids and the corresponding frequency partition.

The decomposition is applied recursively to the low frequency band to obtain the other levels. The whole decomposition can be seen as three oriented N level pyramids $(HH_j, BH_j, HB_j)_{j=1...N}$ with a residual frequency band BB_N. The number of transform samples is equal to the original number because of the orthogonal property . Figure 4 shows the grid representation

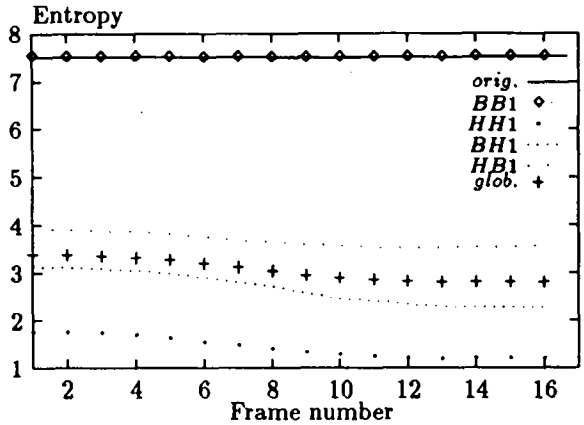

Figure 5: Original, partial and global entropy values computed on 16 "INTERVIEW" frame sequence and on the corresponding 1 level wavelet pyramid sequence.

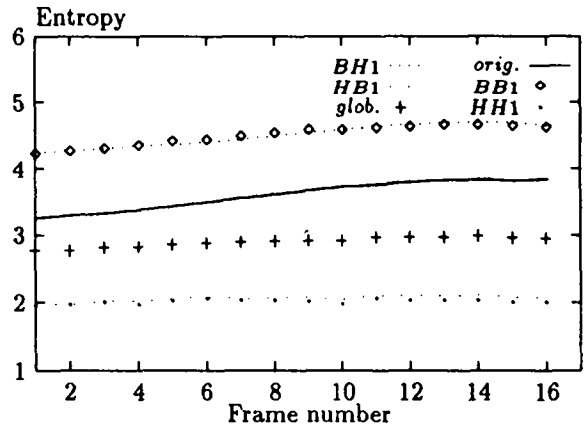

Figure 6: Original, partial and global entropy values computed on the 16 odd "RUBIX" field sequence and on the corresponding 1 level wavelet pyramid sequence.

of the wavelet pyramids in the space domain and the corresponding frequency partition.
The original signal can be perfectly recovered by adding the different interpolated pyramid levels to the residual frequency band (pyramid top). The reconstruction algorithm for 1 level pyramids is described by the following equations :

$$I_0 = \tilde{BB}_1 + \tilde{HH}_1 + \tilde{HB}_1 + \tilde{BH}_1$$

$$\tilde{BB}_1(n,m) = 4\sum_k \sum_l h(n-2k)h(m-2l)BB_1(k,l)$$

$$\tilde{HH}_1(n,m) = 4\sum_k \sum_l g(n-2k)g(m-2l)HH_1(k,l)$$

$$\tilde{HB}_1(n,m) = 4\sum_k \sum_l g(n-2k)h(m-2l)HB_1(k,l)$$

$$\tilde{BH}_1(n,m) = 4\sum_k \sum_l h(n-2k)g(m-2l)BH_1(k,l)$$

where $\tilde{BB}_1, \tilde{HH}_1, \tilde{HB}_1$ and $\tilde{BH}_1$ denote the interpolated versions of BB_1, HH_1, HB_1 and BH_1.
In order to get an idea of the degree of the information decorrelation obtained by this decomposition, we perform a global entropy computation as follow: for a given N level wavelet pyramids, we compute the average of subimage entropies E_j to get the optimal number of bits required per pyramid sample in comparison with an original sample.

$$E_g = \sum_{j=1}^{N} \frac{E_{HH_j} + E_{HB_j} + E_{BH_j}}{2^{2j}} + \frac{E_{BB_N}}{2^{2N}}$$

Original, partial and global entropy values are given in the table below for "INTERVIEW" and "RUBIX" frames and their 2 level wavelet pyramids generated from 4-tap wavelet filters [DAU87] (see figure 18 and 19). Figure 5 and 6 show the stability of this values throw pyramid sequences.

RUBIX frame		INTERVIEW frame	
Original	3.84	*Original*	7.51
E_{BB_2}	4.10	E_{BB_2}	7.47
E_{BH_2}	3.12	E_{BH_2}	3.74
E_{HB_2}	2.34	E_{HB_2}	3.84
E_{HH_2}	2.26	E_{HH_2}	2.87
E_{BH_1}	2.88	E_{BH_1}	2.70
E_{HB_1}	1.89	E_{HB_1}	3.65
E_{HH_1}	1.80	E_{HH_1}	1.42
E_g	2.38	E_g	3.06

Regularity concept :

The wavelet theory and associated multiresolution analysis permit another way, mainly based on mathematical proofs, to interpret some signal processing concepts and leads to some interesting questions such as the regularity of the approximation operator ; indeed, it is important that the infinitely iterated and subsampled lowpass filter converges to some smooth function . I. Daubechies has investigated the regularity of orthonormal wavelet with compact support and a construction has been given for wavelet filters whose regularity increases with the support length [DAU87].

We are interested here to verify if the regularity give us some improvement in the information decorrelation point of view. So, partial and global entropies of pyramid sequences have been computed with different and increasing regularity of the wavelet filters ; then it appears that entropy values are closely similar (see figure 7). In conclusion we can say that there is no significant improvement of entropy criterium when filter regularity increases in comparison with the increase of the computational complexity due to filter support length.

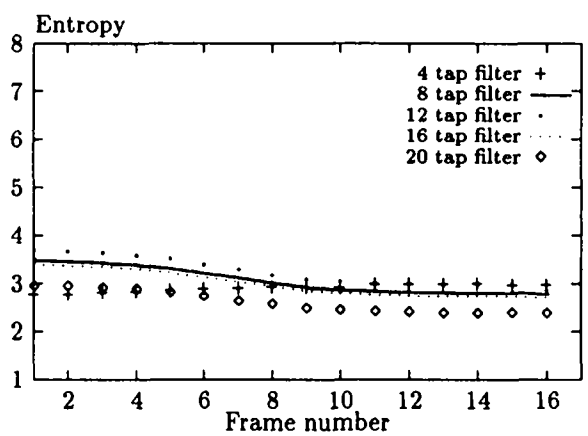

Figure 7: Global entropy values computed at 2 level wavelet pyramids of "INTERVIEW" sequence and obtained for different tap wavelet filters with increasing regularity.

2.4 Quasi-orthogonal pyramid transforms

2.4.1 Introduction

If we use subband coding schemes with filter banks such as Quadrature Mirror Filters [EST77], [WOO86], [VAI87], [ADE87] we only approximate the orthogonality equation and the exact reconstruction property (see section 2.3.2). However, perfect reconstruction schemes with analysis filters different from synthesis filters have been introduced few years ago to improve the QMF performances [VET86], [LE 88], moreover, they have the advantage that short-tap symmetric filters can be used.
Recently, the wavelet theory group developped the mathematical framework of such subband schemes. In this way, the wavelet theory is generalized by constructing biorthogonal wavelet basis (non-orthonormal) and associated multiresolution analysis [DAU90]. Actually, investigations are oriented to the design of symmetric biorthogonal filters close to an orthonormal basis. The regularity problem is investigated in similar manner than in the orthonormal case [DAU90], [ANT90] and [VET90].
To illustrate this class, we have implemented biorthogonal pyramids based on separable filtering and quincunx pyramid based on non-separable QMF filtering. We only detail the family of quincunx representation here and give in the following subsection some implementation details about it.

2.4.2 The quincunx pyramid

This kind of pyramid leads to the representation of an image in a set of subimages that captures information details corresponding to a sequence of resolution ($\sqrt{2}^j$). This transform is especially interesting for the 2-D signals because it is computed using a pair of non-separable analysis/synthesis filters with diamond shape [VET84], [ADE87], [FEA90]. The resulted spectrum partition is finer than in the dyadic case and gives some improvement in terms of spatio-frequency localization. For our implementation, we choose the QMF pair (H, G) proposed in [ADE87]. The corresponding impulse responses are quite symmetric and obey to the following equations :

1- $g(n,m) = (-1)^{n+m} h(n,m)$: quadrature mirror relation.
2- $\sum_n \sum_m h(n,m) = 1$: h is a normalized lowpass kernel.
3- $\sum_n \sum_m g(n,m) = 0$: g is a highpass kernel.

4- $h(|n|,|m|) = h(n,m)$: symmetry relation.

However, orthogonality and exact reconstruction are only approximated.

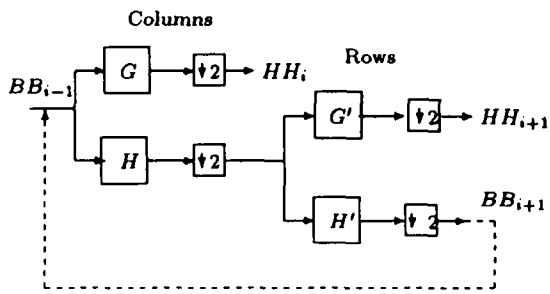

Figure 8: Decomposition diagram of the quincunx pyramid. G' and H' are transformed filters by rotation of 45^0.

As shown in the decomposition diagram of figure 8, the two subbands (lowpass and highpass) obtained after the first step of non-separable filtering are subsampled by a factor of 2 to get quincunx grids. The two subimages size are then reduced to a half of the original size image. At second step, only the lowpass band is splitted, using transformed filters by a rotation of 45^0 followed by quincunx subsampling, into two subimages (highpass and lowpass) defined at rectangular lattices ; indeed two successive quincunx subsampling equal to rectangular one with a factor 4. The two decomposition steps are applied recursively to the lowpass band to obtain the frequency partition of figure 9.
figure 20 shows an example of quincunx pyramid of "INTERVIEW" frame. As in the previous cases, we are interested by entropy computation obtained by such non-separable transform. The global entropy is given by :

$$E_g = \sum_{j=1}^{N} \frac{E_{HH_j}}{2^j} + \frac{E_{BB_N}}{2^N}$$

Note that even if orthogonality is not achieved but only approximated, the pyramid size is equal to the original image size. The table below gives original, partial and global entropies of 5 level quincunx pyramids. We can notice that entropy values are intermediate between the wavelet's values and Laplacian's

3 Motion estimation framework

The general framework for motion estimation that we experimented here is based on well-known pel-recursive differential techniques [NET79], [WAL84], [BIE87]. The basic assumption relating these methods is the temporal invariance of the displaced pel luminances and, in a general way, the recursive estimation procedure can be seen as a minimization of an interframe reconstruction quality criterion. In this paper, we propose an improved recursive procedure which combines the Walker-Rao and the Wiener-based approaches for motion estimation. However, a review of these techniques is of necessity to introduce the modified one.

3.1 Adaptive pel-recursive motion estimation algorithm

This algorithm was introduced by Walker and Rao in 1984 [WAL84]. It uses a steepest descent method to find, for each moving pel p, the optimal motion vector $\hat{d}$ which minimizes the squared displaced frame difference $(DFD)^2$. Let $I(p,t)$ be the intensity value at location $p = (x,y)$ of a moving pel from frame $t-1$ to frame t. Then its DFD is defined as :

$$DFD(p,\hat{d}) = I(p,t) - I(p-\hat{d},t-1)$$

where $\hat{d}$ is its estimated interframe displacement and is given by the following iterative equation :

$$\hat{d}^i = \hat{d}^{i-1} - \Gamma DFD(p,\hat{d}^{i-1}) gradI(p) \tag{1}$$

The update can be controlled by an adaptive gain :

$$\Gamma = \frac{1}{2}\frac{1}{||gradI(p)||^2}$$

Note that i represents the iteration counter and $gradI(p) = (g_x(p), g_y(p))$ the spatial gradient of the luminance I at location $(p-\hat{d}^{i-1})$ in frame $t-1$. The convergence is attained when $|DFD(p,\hat{d}^i)| \leq T$ where T is a given threshold value.

3.2 Wiener-based algorithm

The Wiener-based approach for motion estimation was proposed by Biemond et al. in 1987 [BIE87]. It's a pel recursive technique which provides with a linear least square estimate of the motion vector, for moving pel, using some observations extracted from a space neighbourhood Ω. Assuming that a set Ω of N pels $\Omega = \{(p(1), ..., p(j))_{j=1,2,...,N}\}$ belongs to a moving area, then one can derive N observations by linearizing the DFD function for each pel at the location $(p(j) - d^{i-1})$:

$$DFD(p(1), d^{i-1}) = gradI(p(1))u + v(p(1), d^{i-1})$$

$$\vdots$$

$$DFD(p(N), d^{i-1}) = gradI(p(N))u + v(p(N), d^{i-1})$$

where $v(p(j), d^{i-1})$ denotes the truncation error resulting from the linearization and $u = (d - d^{i-1})$ the update of the previous estimate vector d^{i-1}. Both u and v are considered as samples of stochastic processes. Estimating u is stated as a problem of finding a linear estimator L such that $\hat{u} = Lz$ and $E\{||u - \hat{u}||^2\}$ minimized. In addition of this, u and v are assumed to be orthogonal each other with zero mean value and diagonal covariance matrixes. In this way, Biemond et al. obtain an iterative algorithm to estimate a current pel displacement using a neighbourhood information as described by the equations below :

$$\hat{d}^i = \hat{d}^{i-1} - \begin{bmatrix} \sum_j g_x^2(j) + \mu & \sum_j g_x(j)g_y(j) \\ \sum_j g_x(j)g_y(j) & \sum_j g_y^2(j) + \mu \end{bmatrix}^{-1}$$

$$\begin{bmatrix} \sum_j g_x(j)DFD(p(j), \hat{d}^{i-1}) \\ \sum_j g_y(j)DFD(p(j), \hat{d}^{i-1}) \end{bmatrix} \tag{2}$$

$$1 \leq j \leq N$$

where μ is equal to the ratio of the variance of v and u ($\mu = \frac{\sigma_v^2}{\sigma_u^2}$) and $(g_x(j), g_y(j)) = gradI(p(j))$ represents the spatial gradient of the luminance I at location $(p(j) - \hat{d}^{i-1})$ in frame $t - 1$.

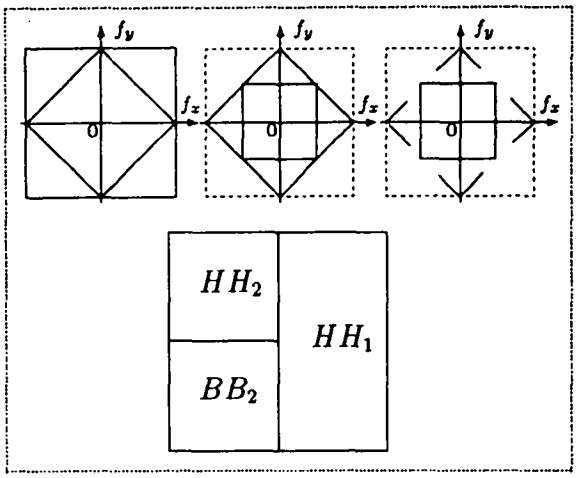

Figure 9: Spatial representation grid of a 3 level quincunx pyramids and the corresponding frequency partition.

values but computations are more complex because of the non-separable filtering.

RUBIX frame			INTERVIEW frame	
Original	3.84		*Original*	7.51
E_{BB_4}	4.13		E_{BB_4}	7.47
E_{HH_4}	3.14		E_{HH_4}	4.30
E_{HH_3}	2.92		E_{HH_3}	3.93
E_{HH_2}	2.87		E_{HH_2}	3.79
E_{HH_1}	2.65		E_{HH_1}	3.36
E_g	2.86		E_g	3.85

2.5 Discussion

Let us remember that all the pyramid representations discussed here have been previously introduced ; however, we thought useful to compare them using a same set of criteria, and summarize them within a unique typology. The main interests of this experimental part is to observe that some pyramidal decompositions provide us with highly compact representation (especially for wavelet and quincunx decompositions), that those performances are

quite stable during a temporal sequence and among several contents of scene. Moreover, if we pay attention to the coherent visual appearance of moving structures when all of theses pyramidal image decompositions are seen in real time along a large TV sequence, it appears attractive to numerically quantify this visual coherence in terms of motion estimations. The following section gives some recalls on the general framework for motion estimation that we propose and subsequent sections describe new motion estimation schemes fitted to pyramidal data structure and motion compensated coding purpose.

3.3 Modified Wiener-based approach

If we reconsider the equations (1) and (2), one can notice that :

- The Wiener algorithm becomes a Walker-Rao algorithm if Ω is restricted to the current pel $N = 1$ and $\mu = 0$.

- Computations required to perform a Walker-Rao iteration are also needed for Wiener-based one.

- Both equations (1) and (2) are usually used with some logic which can be exactly the same.

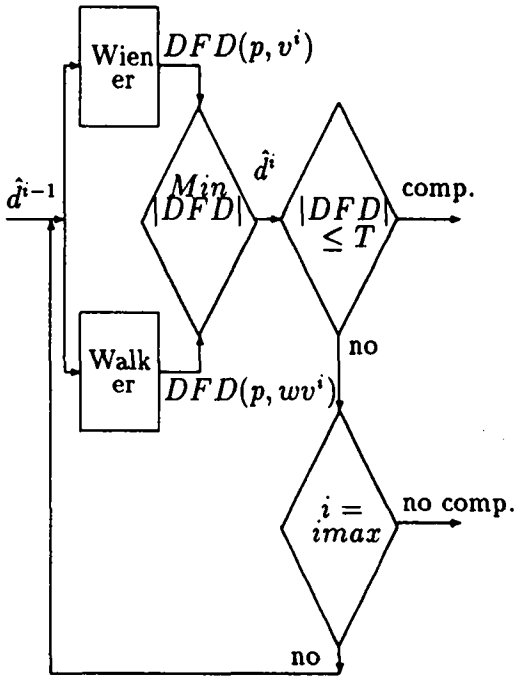

Figure 10: Diagram of the combined Wiener-Walker iteration procedure.

However, the Wiener-based approach works better when the current pel and its neighbourhood belong to a moving object but fails at motion edges and very noisy areas ; therefore, it requires some estimation process without any smoothing effect such as Walker-Rao one. To solve this problem, an improved estimation procedure is developped ; it combines a Wiener-based and a Walker-Rao iterations. One combined iteration step (i) is shown by the diagram in figure 10 and can be described as follows :

- For the initial displacement $\hat{d}^{i-1}$ of the current pel p, we estimate, simultaneously, a Wiener-based update to get a new displacement v^i and a Walker-Rao update to get w^i.

- We compute $DFD(p, v^i)$ and $DFD(p, w^i)$.

- The selected displacement is one whose DFD is smaller. If $|DFD(p, v^i)| \leq |DFD(p, w^i)|$ then $\hat{d}^i = v^i$ else $\hat{d}^i = w^i$.

- Iterations stop when the current pel is compensated $|DFD(p, \hat{d}^i)| \leq T$; however the iteration number is restricted to $imax$ and there will exist some cases for which there is no convergence.

It should be noted that iteration procedure is one part of the motion estimation process which proceeds on a pel-by-pel along the scan direction, as described by the following algorithm :

1) An initial displacement value d^0 is needed to start the iterative process at pel p. It will be one of the displacements found at previous pels, in a causal neighbourhood Ω_{iv}, which gives the smaller $DFD(p, d^0)$ at the current pel. Note that the window of initial values Ω_{iv} is not necessary the same as Ω.

2) *Test1*- If $|DFD(p, d^0)| \leq T$ then $\hat{d} = d^0$. The correct motion displacement is found only by the simple propagation of a previous displacement.

3) *Test2*- Else if $I(p, t) = I(p, t-1)$ then $\hat{d} = 0$. The current pel is not moving.

4) *Test3*- Else use the combined Wiener-Walker procedure to estimate a correct displacement.

If $\sum_{j=1}^{N} |DFD(p(j), d^0)| \leq \sum_{j=1}^{N} |DFD(p(j), 0)|$ then use d^0 to start the iterative procedure else start the iterative procedure with zero value. The iteration process continue until $|DFD(p, \hat{d}^i)| \leq T$ (convergence) or $i = imax$.

5) *Test4*- If the combined Wiener-Walker procedure terminates without any convergence then use a simple Walker-Rao procedure with the initial value d^0 to estimate the correct update.

Modified Wiener-based algorithm		
Parameters	$imax = 20, T = 2, \mu = 5$	
Sequence	RUBIX	INTERVIEW
%no. comp. pels	2.19	2.29
%comp.(Test1)	84.31	69.90
%comp.(Test2)	0.40	0.86
%comp.(Test3)	13.10	26.95
%comp.(Test4)	2.01	3.72
MINCP	6.30	5.20
RMSRE	0.94	0.97

Walker-Rao algorithm		
Parameters	$imax = 20, T = 2$	
Sequence	RUBIX	INTERVIEW
%no. comp. pels	7.45	14.21
%comp.(Test1)	81.71	64.09
%comp.(Test2)	0.34	0.82
%comp.(Test3)	10.50	20.89
MINCP	3.76	3.31
RMSRE	7.09	1.82

Several details have to be adjusted when this algorithm is using such as determining the neighbourhood areas Ω and Ω_{iv}, μ and the threshold value T. Simulations were done using several sequences to determine the optimal choice of theses parameters. The used configurations for Ω and Ω_{iv} are respectively :

```
X X X     X X X
X O       X O
```

where O is the current pel and X a neighbouring one.
After motion estimation process, the original image is reconstructed using the motion prediction :

$$\hat{I}(p,t) = I(p - \hat{d}, t - 1)$$

where $\hat{d}$ is the estimated displacement of the pel p. Motion estimation and reconstruction quality results concerning the "RUBIX" and "INTERVIEW" sequences are given by the table above in terms of percentage of uncompensated pels and compensated ones and the Mean Iteration Number of Compensated Pels ($MINCP$). The Root Mean Squared Reconstruction Error values ($RMSRE$) are also given for the reconstruction error image. One can see that the performances of the combined Wiener-Walker algorithm are quite satisfiying.

4 Multigrid motion estimation

Several previous studies [GLA84], [TER86] have illustrated the efficiency of multigrid strategy within feature estimation processes. To extend motion estimation techniques to hierarchical data structures, such as pyramid transforms, we can also design multigrid motion estimator which should enable cooperation between pyramid levels. Three main problems have to be solved :

1) The choice of the motion estimation algorithm.

2) The choice of the pyramid transform.

3) The design of primitive propagation strategies inside the pyramid representation : coarse-to-fine or somewhat oscillating propagation scheme.

In our case, the primitives will be the motion field, some projection and interpolation operators are defined to controll the information exchange between the pyramid levels. Several previous studies [ENK86], [MIL89] have already experimented these techniques and shown the efficiency of multigrid motion estimation schemes :

- Improvement of estimation efficiency.

- Decrease of the estimation complexity or the number of intermediate computations.

4.1 Multigrid Walker-Rao algorithm on lowpass pyramids

The first hierarchical data representation which we used to investigate a Walker-Rao multigrid algorithm was the lowpass pyramid (see figure 11). The strategy is top-down and can be described by the following algorithm :
1)- Let $(G_0(t-1),...,G_{N-1}(t-1))$ and $(G_0(t),...,G_{N-1}(t))$ the lowpass pyramids of frames $t-1$ and t and let S_0 the original frame size or G_0 size. First, motion estimation is performed between the top pyramid levels $G_j(t-1)$ and $G_j(t)$ with $j = N-1$.
2)- The resulted field $\hat{d}_j$ is interpolated by a factor of 4 to get a size of the finer level $\frac{S_0}{2^{2(j-1)}}$.

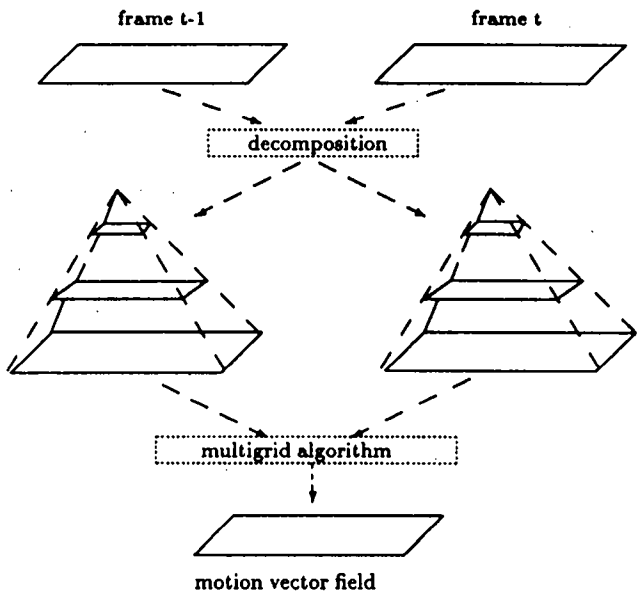

Figure 11: Multigrid approach of motion estimation on lowpass pyramids.

3)- The interpolated motion vectors $\tilde{d}_j$ are matched to the finer pyramid grid $j-1$ and used as initial vector $\hat{d}^0$ for a new motion estimation process. For multiple pyramid levels, the process is repeated until the highest resolution level G_0 is reached.

Simulations show that this strategy improves significantly the motion estimation quality (RMS criterion). Results at "INTERVIEW " frames are given in the table below :

INTERVIEW SEQUENCE		
Parameters	$imax = 20, T = 2$	
pyramid levels	1	0
%no. comp. pels	2.07	2.21
%comp.(Test1)	77.06	75.07
%comp.(Test2)	0.60	0.14
%comp.(Test3)	22.46	24.57
MINCP	5.42	4.84
RMSRE	2.24	1.76

Even if the RMS reconstruction error is quite satisfactory therefore, the computational complexity appears quite similar to a monoresolution approach and this makes an handicap for data compression. It seems promising to use some more compact hierarchical data representation i.e orthogonal or quasi-orthogonal pyramid transform as it is performed in the following section.

4.2 Multigrid Walker-Rao algorithm on wavelet pyramids

The second multigrid strategy associated to the Walker-Rao algorithm is related to the wavelet pyramids. This choice is very attractive in the point of view of computation complexity because it takes advantages of the compactness of available data. However, the particular properties of orientation and frequency partition of the wavelet transform makes the associated multigrid strategy different and more complicated.

First, assuming that we have four motion fields $\hat{d}(HH_1), \hat{d}(HB_1), \hat{d}(BH_1)$ and $\hat{d}(BB_1)$ corresponding to the four subbands of one level wavelet pyramids, there will be two ways to reconstruct the original image :

a) by merging the four motion fields to get one field which predict correctly the original image.

b) by using the wavelet reconstruction algorithm with the predicted subbands $\hat{HH}_1, \hat{HB}_1, \hat{BH}_1$ and $\hat{BB}_1$.

In (a) the main difficulty is to design an efficient merging method, some heuristic procedures such as linear combinations have been tested and results were without success. In case of (b) only reconstruction errors of pyramid levels can affect the global reconstruction quality.

Secondly, one can ask how to estimate the four motion fields. There are two possibilities :

c) we can use a simple Walker-Rao algorithm in each subband. In this case, one level wavelet pyramids are sufficient.

d) we can introduce multigrid estimation, as in lowpass pyramids, along each oriented N level wavelet pyramid to improve the motion field quality. Two strategies are shown in figure 12 and 13.

If $\hat{d}(BB_1)$ is estimated directly from BB_1, the amount of involved data exceeds the available one in the wavelet pyramids, else if $\hat{d}(BB_1)$ is derived from the top pyramid level BB_N then it involves some merging procedure. Finally, one can say that a Walker-Rao multigrid algorithm on wavelet pyramid suffers from the unavailability of efficient merging operators. Moreover, the data compression requirements makes the problem more complex. Because of all these desagrements, we retire this strategy in favour of a method which includes implicitely merging operators. The multiconstraint framework described in the next section provides us with such an algorithmic tool.

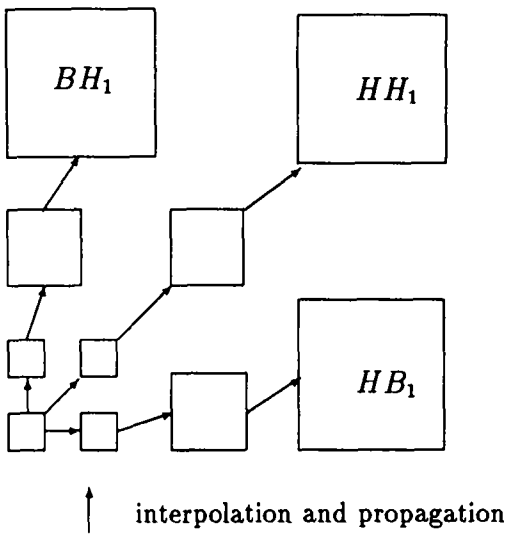

Figure 12: Multigrid strategy on 3 level wavelet pyramids.

5 Multiconstraint algorithm

In the context of image sequence codecs where real-time constraints are very heavy, the critical algorithmic step in terms of computation amount is essentially the motion estimation process. So in this method, the basic assumption, when several frequency-oriented subbands are used is that only one motion vector field can be estimated and validated at all decomposition levels. We assume indeed that spatio-frequency localization properties are compatible with correlated motion attributes. From an algorithmic point of view, the main difficulty is to design an efficient merging procedure to estimate the motion vector of moving pel from several frequency bands simultaneously.
The solution that we propose is to use the combined Wiener-Walker algorithm with a multiresolution neigbourhood Ω_m. As in the usual Wiener approach where a spatial coherence is assumed for motion vector field, we suppose that a frequential coherence exists and can be useful to motion estimation efficiency. This last assumption appears quite reasonable because for pixels related to frequency components of the same moving object are related to the same motion displacement vector. By this way, we essentially use the avai-

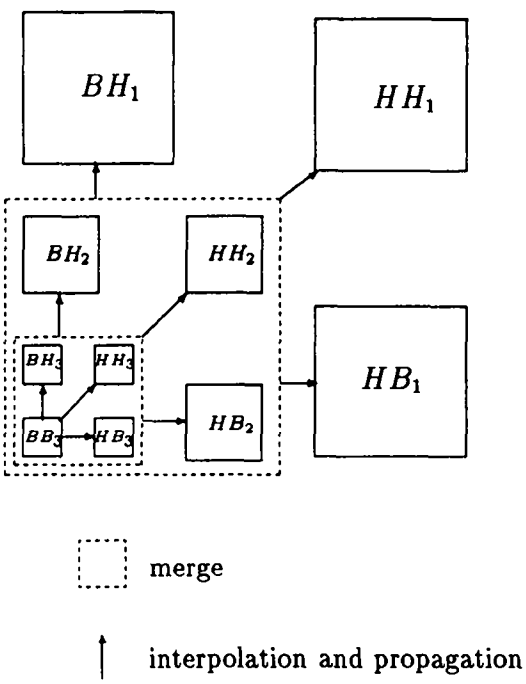

Figure 13: Multigrid strategy on 3 level wavelet pyramids.

lable spatio-frequency localization of pyramid transforms to solve the initial and crucial merging problem.

Some simplifications are introduced to facilitate implementation complexity and then simultaneous combination includes only the levels which have the same size grid.

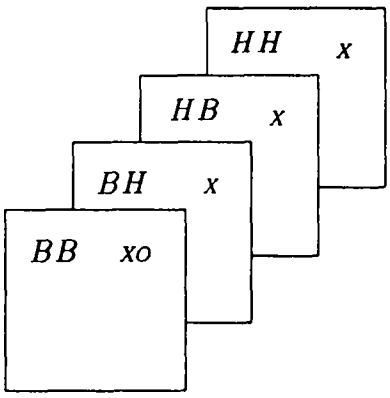

Figure 14: Multiresolution neibourhood configuration Ω_m.

So N observations will be extracted from four subbands to estimate a reliable displacement for the entire Ω_m. Assuming that we need to estimate the correct displacement of a pel p, the set Ω_m will contain $\Omega = \{BB_1(p), HH_1(p), BH_1(p), HB_1(p)\}$ and all the tests of the estimation process will acts at $BB_1(p)$. The resulted displacement is used to predict all Ω because the four points are related to frequency components of the same moving object. Let us notice that :

- To make easy the comparison between the combined Wiener-Walker algorithm (spatial neighbourhood of 5 points) and the multiconstraint algorithm, we choose a multiresolution neighbourhood Ω_m with 5 points as shown in figure 14.
- The multiconstraint algorithm decreases the computation complexity in comparison to the combined Wiener-Walker applied to an original image because it works at $\frac{S_0}{4}$ image size and each iteration includes 5 pels.

- The resulted motion field is used to predict the four subbands $\hat{BB}_1, \hat{HH}_1$, $\hat{BH}_1, \hat{HB}_1$ and the original image is reconstructed by the wavelet reconstruction algorithm.
- The estimation process is concentrated at the lowpass frequencies (BB_1) since it represents the context of the image and contains much more information (see entropy values in section 2.3).

Results are given by the table below; the main important concluding remark is to observe that, for quite similar (even better) reconstruction quality ($RMSRE$ criterion) and motion compensation efficiency (% no-compensated pel number), the use of multiresolution neighbourhood in comparison to a spatial one enables a faster convergence (see $MINCP$ values) of the recursive motion estimator and highly decreases the computational complexity (here in a percentage of nearly 30%). Moreover, if some less critical set of parameters ($imax, T$ ...) would be tested, we should observe an even more distinguishable behaviour of these two approaches in favour of the multiconstraint method.

Parameters	$imax = 20, T = 2, \mu = 5$	
Algorithm	Wiener-Walker	Multiconst.
Sequence	INTERVIEW (BB_1)	
%no. comp.	2.50	2.28
%comp.(Test1)	72.43	72.10
%comp.(Test2)	0.78	0.80
%comp.(Test3)	24.29	24.83
%comp.(Test4)	3.87	2.35
$MINCP$	6.03	4.62
$RMSRE(BB_1)$	1.46	1.37

We want also to compare respectively the original image reconstruction quality between a monoresolution motion compensation approach (see table of subsection 3.2) and a multiconstraint algorithm (see table below). In both cases, a high quality (respectively for "INTERVIEW" sequence, the $RMSRE$ is 0.97 and 2.27) is achieved, with no perceptible reconstruction artefacts. Moreover, the efficiency of motion compensation is quite similar (see %no-comp. : i.e for "INTERVIEW" 2.29 in the monoresolution case, 2.28 in the multiconstraint case). The main advantage of the multiconstraint algorithm is that it works only on a $\frac{S_0}{4}$ image size.

Figure 21 shows the prediction error images, we could observe the high quality of reconstruction, especially in comparison to the temporal difference images (see figure 15 and 16).
This multiconstraint algorithm may be extended to the lower pyramid levels by the design of multigrid strategy, and is presently subject to promising results.

Multiconstraint algorithm		
Parameters	$imax = 20, T = 2, \mu = 5$	
Sequence	RUBIX	INTERVIEW
%no. comp.	1.60	2.28
%comp.(Test1)	83.78	72.10
%comp.(Test2)	0.52	0.80
%comp.(Test3)	14.10	24.83
%comp.(Test4)	1.58	2.35
$MINCP$	5.48	4.62
$RMSRE(BB_1)$	0.35	1.37
$RMSRE(HH_1)$	0.95	1.08
$RMSRE(HB_1)$	0.91	1.23
$RMSRE(BH_1)$	3.03	1.47
RMSRE recons.	2.98	2.27

6 Discussion

For television sequence coding, pel-recursive motion techniques have been investigated using a monoresolution data structure. In this study, we have implemented several multiresolution structures to evaluate them using the same criteria. As concluding remarkes, we can say with no doubt, that orthogonal transforms (especially wavelet pyramids or quincunx pyramids) provide us with a more compact representation in a spatial point of view. However, these methods need efficient merging operators to estimate a unique feature (motion in our case) field along the different frequential subbands and to reduce the computational complexity. A combined Walker-Rao and Wiener-based approach gives a natural algorithmic framework to implement such a multiconstraint algorithm. The results on real TV sequences validate this method giving for a perfect quality of reconstruction (needed to broadcast quality) a decreasing of amount motion estimates : only an estimation field upon size

of $\frac{S_0}{4}$ (if S_0 denotes the original image size) is needed when a multiconstraint method at one pyramidal level is used ; as further researches seem to prove, we can also introduce multigrid-multiconstraint approach using several pyramidal levels given a more smoothed motion field for an estimation surface of $\frac{S_0}{3}$.

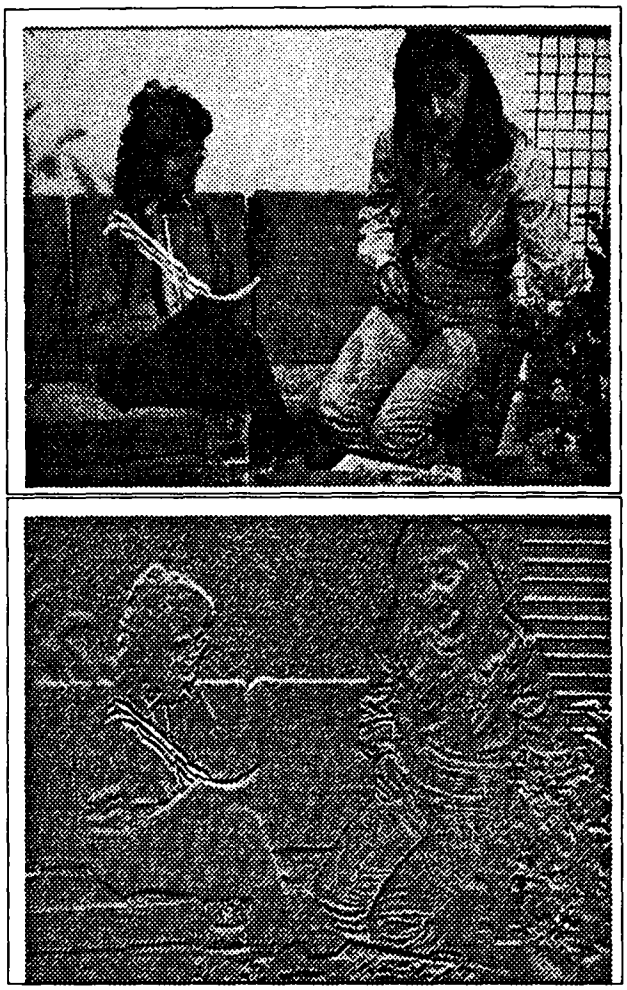

Figure 15: One of two successive original frames of "INTERVIEW" sequence and their temporal difference image. The Root Mean Square (RMS) of the difference image equals to 16.80.

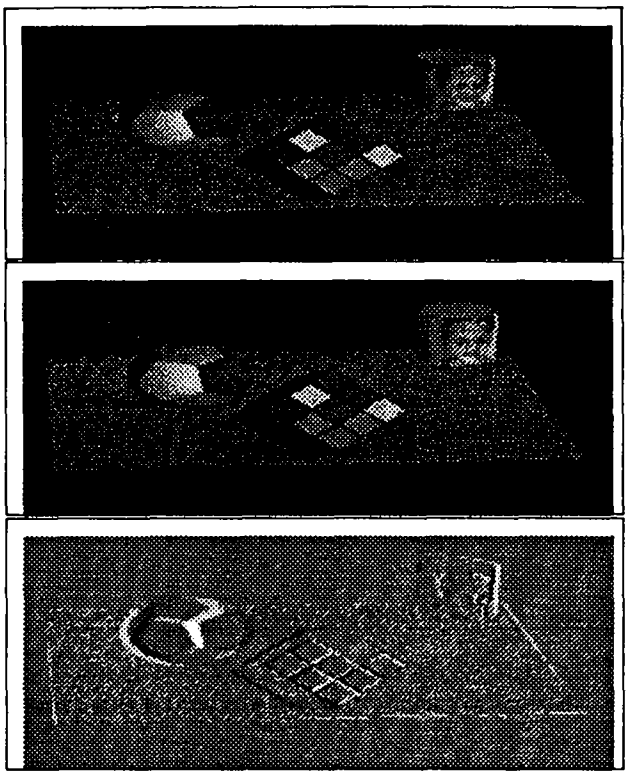

Figure 16: Two original fields of "RUBIX" sequence and their temporal difference image. The root mean square (RMS) of the difference image equals to 10.60.

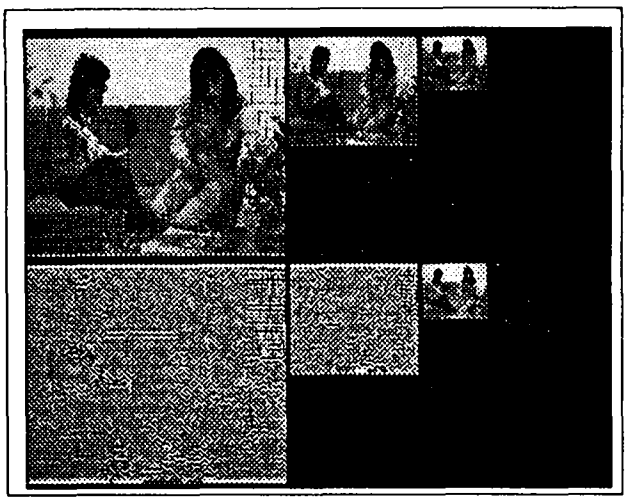

Figure 17: 3 level pseudo-Gaussian and pseudo-Laplacian pyramids of "INTERVIEW" frame obtained by using 9-tap lowpass filter extracted from a QMF pair.

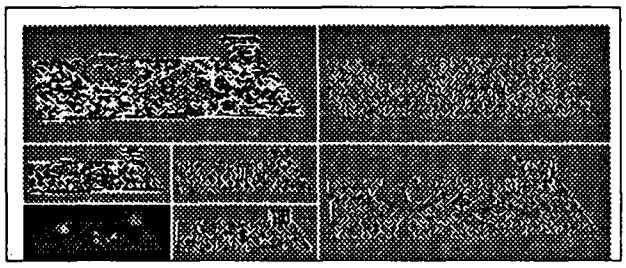

Figure 18: 2 level wavelet pyramids of "RUBIX" field generated with 4-tap wavelet filters.

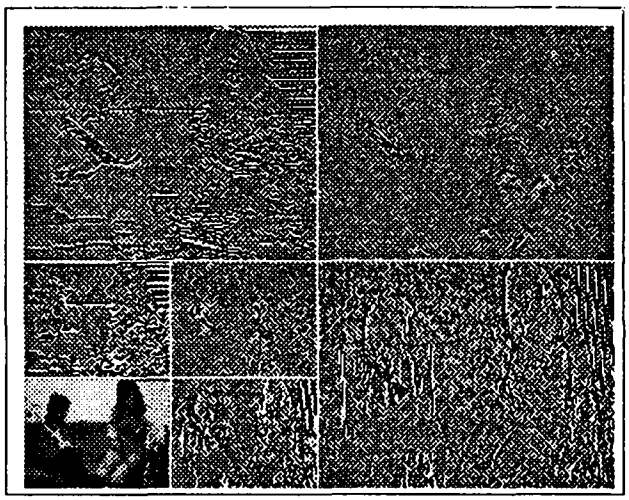

Figure 19: 2 level wavelet pyramids of "INTERVIEW" frame generated with 4-tap wavelet filters.

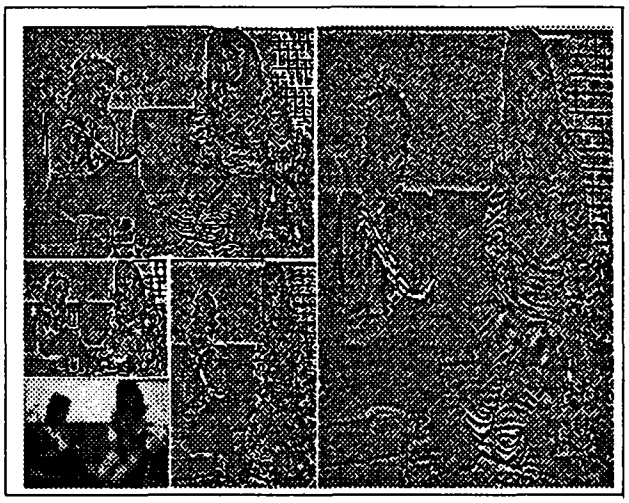

Figure 20: 5 level quincunx pyramid of "INTERVIEW" frame.

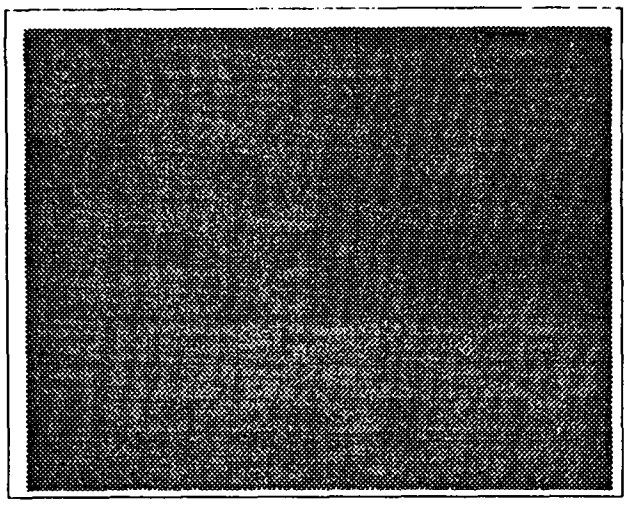

Figure 21: Prediction error image resulting from the compensation of an original frame of "INTERVIEW'" sequence by the multiconstraint algorithm.

References

[ADE87] ADELSON E. and SIMONCELLI E. Orthogonal pyramid transforms for image coding. In *Proc. of the SPIE Conf. on Visual Communications and Image Processing*, pages 50–58, 1987.

[ANT90] ANTONINI M., BARLAUD M., MATHIEU P. and DAUBECHIES I. Image coding using vector quantization in the wavelet transform domain. In *International Conference on Acoustic, Speech and Signal Processing*, pages 2297–2300, Albuquerque, New Mexico, April 1990.

[BAA90a] BAAZIZ N. and LABIT C. Laplacian pyramid versus wavelet decomposition for image sequence coding. In *International Conference on Acoustic, Speech and Signal Processing*, pages 1965–1968, Albuquerque, New Mexico, April 1990.

[BAA90b] BAAZIZ N. and LABIT C. *Transformations pyramidales d'images numériques.* Technical Report 526, IRISA/INRIA, Rennes, Mars 1990.

[BIE87] BIEMOND J. , LOOIJENGA L. and BOEKEE D.E. A pel recursive wiener-based displacement estimation algorithm. *Signal Processing*, 13:399–412, 1987.

[BUR83] BURT P.J. and ADELSON E. The laplacian pyramid as a compact image code. *IEEE Transactions on Communications*, 31:532–540, April 1983.

[DAU87] DAUBECHIES I. *Orthonormal bases of compactly supported wavelets.* Technical Report, AT&T Laboratories, USA, 1987.

[DAU90] DAUBECHIES I., COHEN A. and FEAUVEAU J. C. *Biorthogonal bases of compactly supported wavelets.* Technical Report, AT&T Laboratories, USA, 1990.

[ENK86] ENKELMANN W. Investigations of multigrid algorithms for the estimation of optical flow fields in image sequences. In *IEEE Workshop on Motion: Representation and Analysis*, Charleston, May 1986.

[EST77] ESTEBAN D. and GALAND C. Application of quadrature mirror filters to split band voice coding systems. In *International Conference on Acoustic, Speech and Signal Processing*, pages 191–195, Washington, USA, May 1977.

[FEA90] FEAUVEAU J.C. *Analyse multirésolution par ondelettes non orthogonales et bancs de filtres numériques.* PhD thesis, Université Paris-Sud, Janvier 1990.

[GLA84] GLAZER F. *Multiresolution image processing analysis: Multilevel relaxation in low-level computer vision. Information Sciences*, Springer-Verlag, 1984.

[LE 88] LE GALL D. and TABATABAI A. Sub-band coding of digital images using symmetric short kernels and arithmetics coding

techniques. In *IEEE Transactions on Acoustic, Speech and Signal Processing*, pages 761–764, 1988.

[MAL89] MALLAT S.G. A theorie for multiresolution signal decomposition: The wavelet representation. *IEEE Transactions on Pattern Analysis and Machine Intelligence*, 11(7):674–693, July 1989.

[MEE87] MEER P., BAUGHER E. S. and ROSENFELD A. Frequency domain analysis and synthesis of image pyramid generating kernels. *IEEE Transactions on Pattern Analysis and Machine Intelligence*, 9(4):512–522, July 1987.

[MEY87] MEYER Y. Ondelettes, fonctions splines et analyses graduees. In *Rend. Sem. Mat.*, page 45(1), Universite Polytechniques de Torino, 1987.

[MIL89] MILLOUR C. *Contribution a la vision dynamique : une approche multi-resolutions et multi-traitements.* PhD thesis, Université de Paris-Sud, France, Mars 1989.

[NET79] NETRAVALI A.N. and ROBBINS J.D. Motion compensated television coding-part 1. *Bell System technical Journal*, 58(3):629–668, 1979.

[SJO86] SJOBERG F. *Laplacian pyramids : experiments with a multiresolution image representation.* Technical Report NA-E 8569, IRITA, Department of Numerical Analysis and Computing Science, Royal Institute of Technology S-10044 Stockholm, Sweden, January 1986.

[SMI86] SMITH M. and BARNWELL T. Exact reconstruction echniques for tree structured subband coders. *International Conference on Acoustic, Speech and Signal Processing*, 34(3):434–441, June 1986.

[TER86] TERZOPOULOS D. Image analysis using multigrid relaxation methods. *IEEE Transactions on Pattern Analysis and Machine Intelligence*, 8(2):129–139, March 1986.

[VAI87] VAIDYANATHAN P.P. . Quadrature mirror filter banks, m band extensions and perfect-reconstruction techniques. *IEEE Magazine on Acoustic Speech and Signal Processing*, 4:4–20, July 1987.

[VET84] VETTERLI M. Multi-dimensional subband coding : some theory and algorithms. *Signal Processing*, 6:97–112, 1984.

[VET86] VETTERLI M. Filter banks allowing perfect reconstruction. *Signal Processing*, 10:219–244, 1986.

[VET90] VETTERLI M. Wavelets and filter banks : relationships and new results. In *International Conference on Acoustic, Speech and Signal Processing*, pages 1723–1726, Albuquerque, New-Mexico, April 1990.

[WAL84] WALKER D. R. and. RAO K. R. Improved pel-recursive motion compensation. *IEEE Transactions on Communications*, 32(10):1128–1134, October 1984.

[WOO86] WOOD J.W. and O'NEIL S. Subband coding of images. *IEEE Transactions on Acoustic Speech and Signal Processing*, 34(5):1278–1288, October 1986.

LISTE DES DERNIERES PUBLICATIONS INTERNES IRISA

1990 :

PI 560 A SIMPLE TAXONOMY FOR DISTRIBUTED MUTUAL EXCLUSION ALGORITHMS
Michel RAYNAL
Novembre 1990.

PI 561 MULTIMODAL ESTIMATION OF DISCONTINOUS OPTICAL FLOW USING MARKOV RANDOM FIELDS
Fabrice HEITZ, Patrick BOUTHEMY
Novembre 1990, 50 Pages.

PI 562 EFFICIENT GLOBALCOMPUTATIONS ON A PROCESSOR NETWORK WITH PROGRAMMABLE LOGIC
J M. FILLOQUE, E. GAUTRIN, B POTTIER
Novembre 1990, 14 pages.

PI 563 EQUATIONAL SETS OF TREE-VECTORS
Anne GRAZON, Jean-Claude RAOULT
Novembre 1990, 20 Pages.

PI 564 MULTIFRAME-BASED IDENTIFICATION OF MOBILE COMPONENTS OF A SCENE WITH A MOVING CAMERA
Edouard FRANCOIS, Patrick BOUTHEMY
Décembre 1990, 30 pages.

PI 565 NAIVE RESERVE CAN BE LINEAR
Pascal BRISSET, Olivier RIDOUX
Novembre 1990, 18 pages.

PI 566 METHODES D'INTEGRATION TEMPORELLE EN TRAITEMENT D'ANTENNE
Olivier ZUGMEYER, Jean-Pierre LE CADRE
Décembre 1990, 54 pages. Rapport n° 1

PI 567 METHODES PARAMETRIQUES POUR LA DETECTION DE SOURCES EN MOUVEMENT [1]
Olivier ZUGMEYER, Jean-Pierre LE CADRE
Décembre 1990, 42 pages. Rapport n° 2

PI 568 QUOI RETENIR D'UN ARBRE DE CLASSIFICATION ? UN ESSAI EN QUANTIFICATION D'IMAGE NUMERISEE
Israël César LERMAN, Nadia GHAZZALI
Décembre 1990, 36 pages, Projet CADO.

PI 569 VARIABLES RELATIONNELLES CODAGE ET ASSOCIATION
Mohamed OUALI ALLAH
Décembre 1990, 40 pages

1991 :

PI 570 DESIGN DECISION FOR THE FTM : A GENERAL PURPOSE FAUTL TOLERANT MACHINE
Michel BANATRE, Gilles MULLER, Bruno ROCHAT, Patrick SANCHEZ
Janvier 1991, 30 pages

PI 571 ANIMATION CONTROLEE PAR LA DYNAMIQUE
Georges DUMONT, Parie-Paule GASCUEL, Anne VERROUST
Février 1991, 84 pages

PI 572 MULTIGRID MOTION ESTIMATION ON PYRAMIDAL REPRESENTATIONS FOR IMAGE SEQUENCE CODING
Nadia BAAZIZ, Claude LABIT
Février 1991, 48 pages

ISSN 0249-6399